INNOVATIVE CONTACT JOINTS FOR COMPRESSION STRUTS OF WIDE SPAN WOODEN TRUSS GIRDERS

INNOVATIVE KONTAKTVERBINDUNGEN FÜR DRUCK-STREBEN WEITGESPANNTER HOLZ-FACHWERKTRÄGER

Lisa Stimpfle[1], Jan L. Wenker[2], Gerhard Dill-Langer[1]

[1] *Materials Testing Institute (MPA), University of Stuttgart, Otto-Graf-Institute*

[2] *Brüninghoff Group, Heiden*

SUMMARY

The paper reports on investigations into optimized multiple-step contact joints for use as compression diagonal connections in nodes of new types of timber trusses. In contrast to conventional step joint geometries, the depth of the individual steps in the modified connections is changed continuously over the length of the connection. By means of specially developed compression-shear tests on full-scale specimens, the influence of the modified connection geometries on the load-bearing capacity of connections between glulam (glued laminated timber) and GLVL (glued laminated veneer lumber) is characterized. The test results show an increase in the load-bearing capacity of the modified multiple step joint compared to the standard variant by about 20 %, which can be explained by the activation of several shear surfaces in the laminated veneer lumber resulting additionally in reduction of strength spread.

ZUSAMMENFASSUNG

Der Artikel behandelt Untersuchungen an optimierten Treppenversatz-Verbindungen für den Einsatz als Druckdiagonalen-Anschlüsse in Knotenverbindungen von neuartigen Holz-Fachwerkträgern. Abweichend von üblichen Treppenversatz-Geometrien werden bei den modifizierten Anschlüssen die Tiefe der einzelnen Versätze kontinuierlich über die Verbindungslänge variiert. In speziell hierfür entwickelten Druck-Scherversuchen an vollmaßstäblichen Verbindungen wird der Einfluss der modifizierten Anschlussgeometrien auf die Tragfähigkeit einer

Verbindung von Brettschichtholz mit GLVL (verklebten Furnierschichtholz) charakterisiert. Die Versuchsergebnisse zeigen eine Erhöhung der Tragfähigkeit der modifizierten Treppenversätze gegenüber der Standard-Variante um etwa 20 %, was durch die Aktivierung mehrerer Scherflächen im Furnierschichtholz erklärt werden kann und zusätzlich auch zu einer Reduktion der Festigkeitsstreuungen führt.

1. INTRODUCTION

Contact connection have a long history in timber structures. Today, advancements in computer-aided processing and the ability to create precise, highly detailed connections offer significant opportunities to optimize existing standard geometries. Especially, with the increasing focus on circularity of resources, the easy separability of assembled contact connections is highly relevant.

Among the various types of contact connections, multiple step joints are becoming increasingly important due to the advancements in processing. These joints represent an evolution of the classical single or double step joints. The primary advantage of a multiple step joint is its ability to use the entire connection length for load transfer, which results in a higher load-bearing capacity compared to classic step joints [3] and a more efficient, centered load introduction. Furthermore, the geometry of multiple step joints can be easily adapted to varying connection angles, offering flexibility in structural design.

The contact connection presented in this paper is part of a truss node, designed as a part of a research project by the company Brüninghoff Holz GmbH & Co. KG, Heiden, together with the MPA, University of Stuttgart. The objective of this project is to develop a lightweight truss construction with bonded and contact joints. The contact connection is realized as a multiple step joint. Optimized geometries are investigated to enhance the load-bearing capacity and redundancy of the connection. A corresponding test method was developed to evaluate these geometries and to determine the load capacity of the connections.

2. DESCRIPTION OF THE INNOVATIVE CONTACT JOINT AND THE SPECIMEN LAYUP

The developed truss consists of twin chords with bonded tension diagonals in between. The connection between tension and compression diagonal is realized through a contact connection, in form of a multiple step joint. This ensures an

intersection of the acting forces of the individual components in a single point, reducing internal moments due to eccentricities. (see Fig. 1)

Previous, quasi multiaxial tests on full-size truss joints were performed to examine the load bearing behavior of the truss nodes. For these tests the contact connection between tension and compression diagonal was designed as a multiple step joint with a constant embedment depth. For specimens with a tension diagonal made of glued laminated veneer lumber (GLVL) from spruce, failure consistently occurred in the contact connection. In particular, shear failure in the tension diagonal was observed mainly occurring in one single veneer layer at the bottom of the steps.

To prevent failures in a single layer and to provide more redundancy in the connection, the geometry of the standard multiple step joint with an embedment depth of t_v = 15 mm (in the following called “Standard”) was optimized. Therefore, two alternative geometries of the step joint (in the following called “Modified 1 and 2”) with altering embedment depths of the individual steps, aiming at an activation of several layers of the LVL, were developed. The individual width of each step was chosen proportional to the varying embedment depth of the respective step. “Modified 1 and 2” consist of a joint with 8 or 6 steps and a maximum embedment depth of t_v = 57 mm or t_v = 70 mm, respectively. In both versions, the gradation between the individual steps is 6 mm. All variations are shown in Fig. 2.

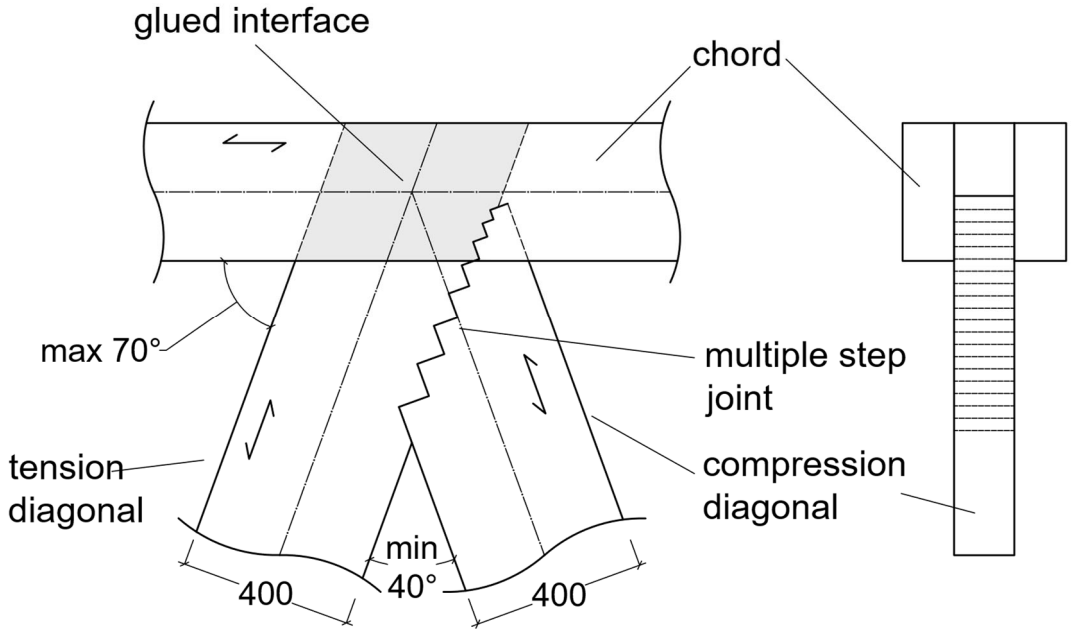

Fig. 1: Sketch of the novel timber truss node with contact connection between compression and tension diagonals and a glued connection between tension diagonal and chords

The specimens tested consist of a tension diagonal made of spruce GLVL (from Kerto S laminations) according to Z-9.1-847 [1] connected to solid wood glulam made from spruce (GLT), strength class GL24h according to DIN EN 14080 [2], both with cross-sectional dimensions of 400 mm x 120 mm. The two components are connected with an angle of 40° between the fiber directions by means of the sketched versions of multiple step joints. For transport and installation, the two components are fixed by means of two screws, however without any load-bearing purpose. The selected angle of 40° between the compression and tension diagonals is equivalent to the tested angle in the full-size joint tests, corresponding to the smallest angle occurring in the area of the edge nodes, which results from the planned geometry of the truss girder.

To take into account the potential shear reinforcement of the tension diagonal by the glued-on chords in an actual truss node, additional sections of GLT made from spruce of strength class GL 24h with a material thickness of 120 mm were glued on. The protruding timber length results from the geometry of the joints of the truss (see Figs. 5 and 6 for a side view of the specimen mounted in the test set-up). Three series – comprising between 4 and 6 test specimens – with different geometries of the multiple step joint, as described above, were tested.

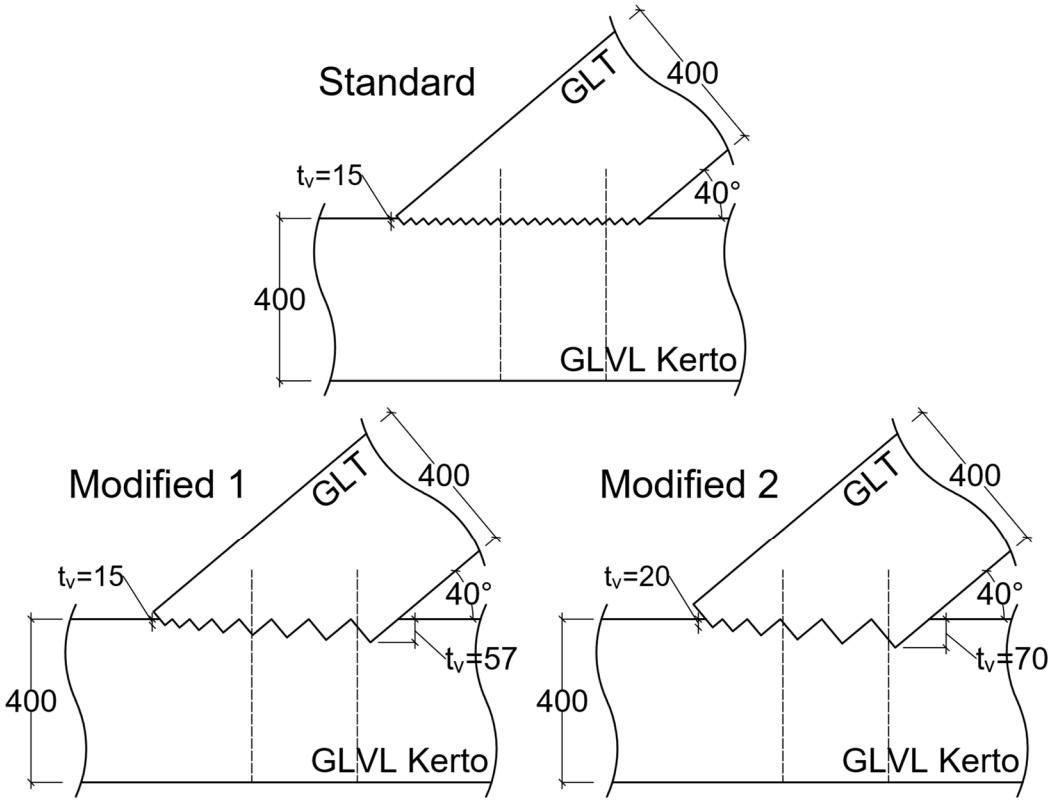

Fig. 2: Investigated geometries of the contact step joint

3. DEVELOPMENT AND DESIGN OF EXPERIMENTAL SETUP

A test setup was designed to evaluate the load-bearing capacity of multiple step joints, with a particular focus on the occurring shear stresses. It is based on a test setup presented in [3]. In the actual load distribution of the investigated truss node, the tension diagonal would normally be subjected to tension forces. However, due to significant effort required to support the specimens by anchoring tension forces, it was decided to perform compression tests instead. This decision was based on a modelling-based analysis, evaluating the impact of a compression and tension support on the shear stresses within the area of the multiple step joint.

3.1 Modelling-based development of the experimental setup

The parametric 2D finite element (FE) model of the tested configuration was created with the commercial software Abaqus v2023 [4] using its Python API. The models with compression- and tension-based support are shown in Fig. 3a and b. The boundary conditions were defined based on the experimental setup. Constraints were applied to the bottom end face and longitudinal side of the structure, limiting movement perpendicular to the respective edges of the tension diagonal. A vertical load was applied to the upper end of the compression diagonal.

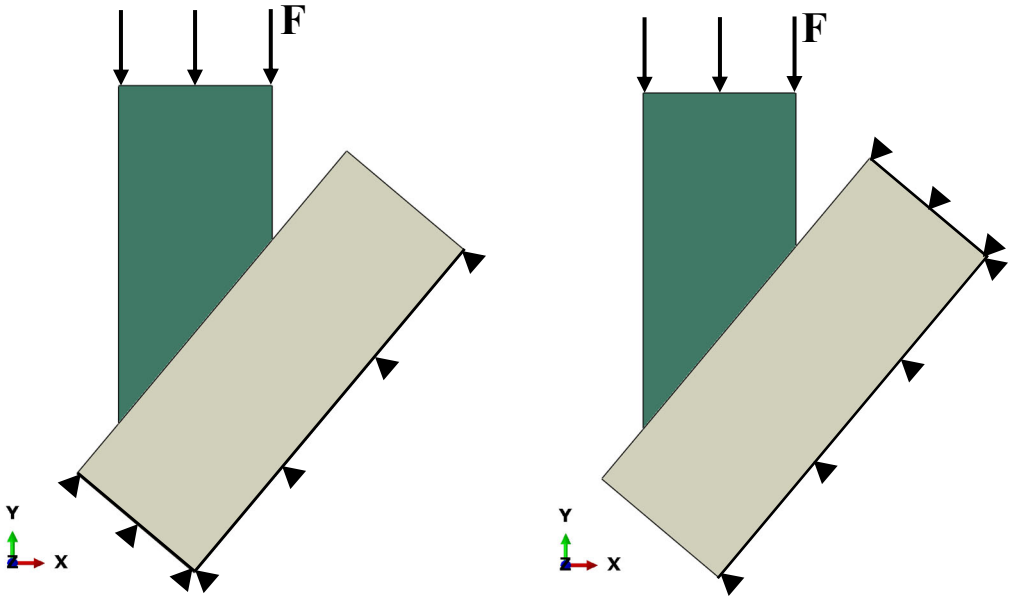

Fig. 3: Finite element model of the experimental setup with compression (a) and tension-based support (b)

The connection between the compression and tension diagonal components was simplified, modeled as a planar surface without detailed geometry of the individual steps. The connection was realized with a contact behavior allowing separation after contact. The material properties were defined according to [2] and [6]. Linear elements were used to mesh the geometry with a maximum element size of 10 mm.

Assuming that the shear stresses in the tension diagonal along the connection are responsible for failure, these stresses were focused in this analysis. Fig. 4 illustrates the shear stress distribution under both compression- and tension-based loading conditions. In both cases, a stress concentration is observed at the lower end of the connection, with nearly identical maximum values and a qualitatively similar stress distribution across the entire area. This indicates no significant differences in shear stress distributions along the multiple step joint.

Thus, it was concluded that the compression shear stresses fully reflect the real (tensile shear tests) with respect to shear stress loading.

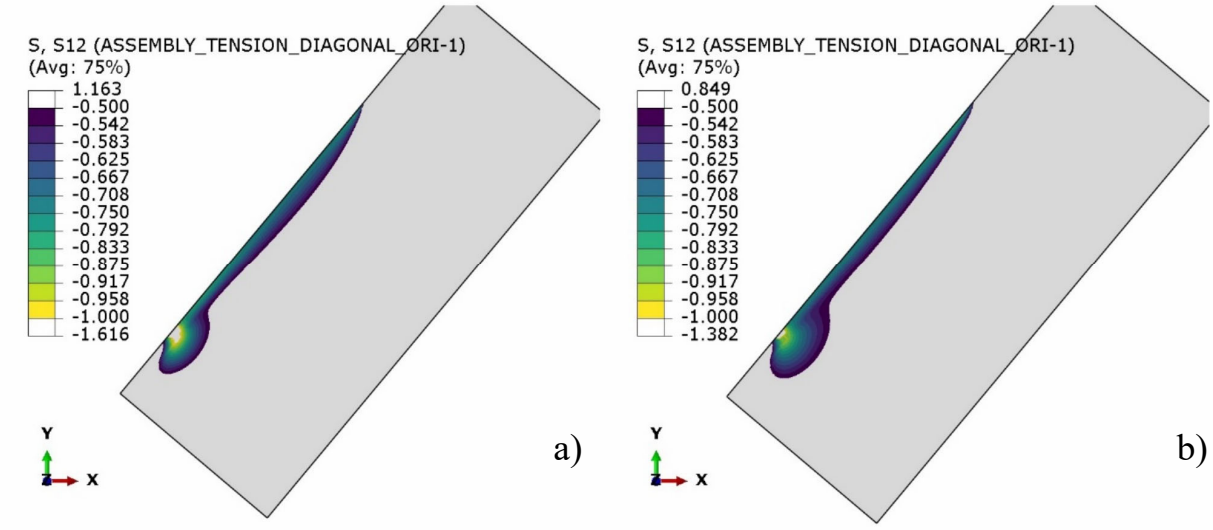

Fig. 4: Shear stresses over the length of the connection with compression (a) and tension-based support (b)

3.2 Experimental setup

The test setup is shown in Fig. 5. The tests were carried out using a rigid welded steel frame (angle 90° between the two edges), which was rigidly connected to the base plate at an angle of 50°. This test layup allowed a tested angle between tension and compression diagonal of 40°, which is the most unfavorable, in the truss possible angle with respect to the shear stress. The tension diagonal is

aligned and supported by the steel frame to ensure it is constraint by both the end grain face and the longitudinal face. In order to eliminate influences from friction and thereby to avoid transversal tension stresses at the end face, a double layer of Teflon and additional steel plates are placed between the test specimen and the steel frame.

The compression load was applied to the end-grain face of the compression diagonal parallel to fiber direction. In combination with the support of the tension diagonal this results in compression forces in both components, compression and tension diagonal. However, to facilitate the identification of the components, the supported component will continue to be referred to as the "tension diagonal".

The tests were carried out by ramp-loading in a servo-hydraulic testing machine in displacement-controlled mode until failure. The realized test setup is shown in Fig. 6.

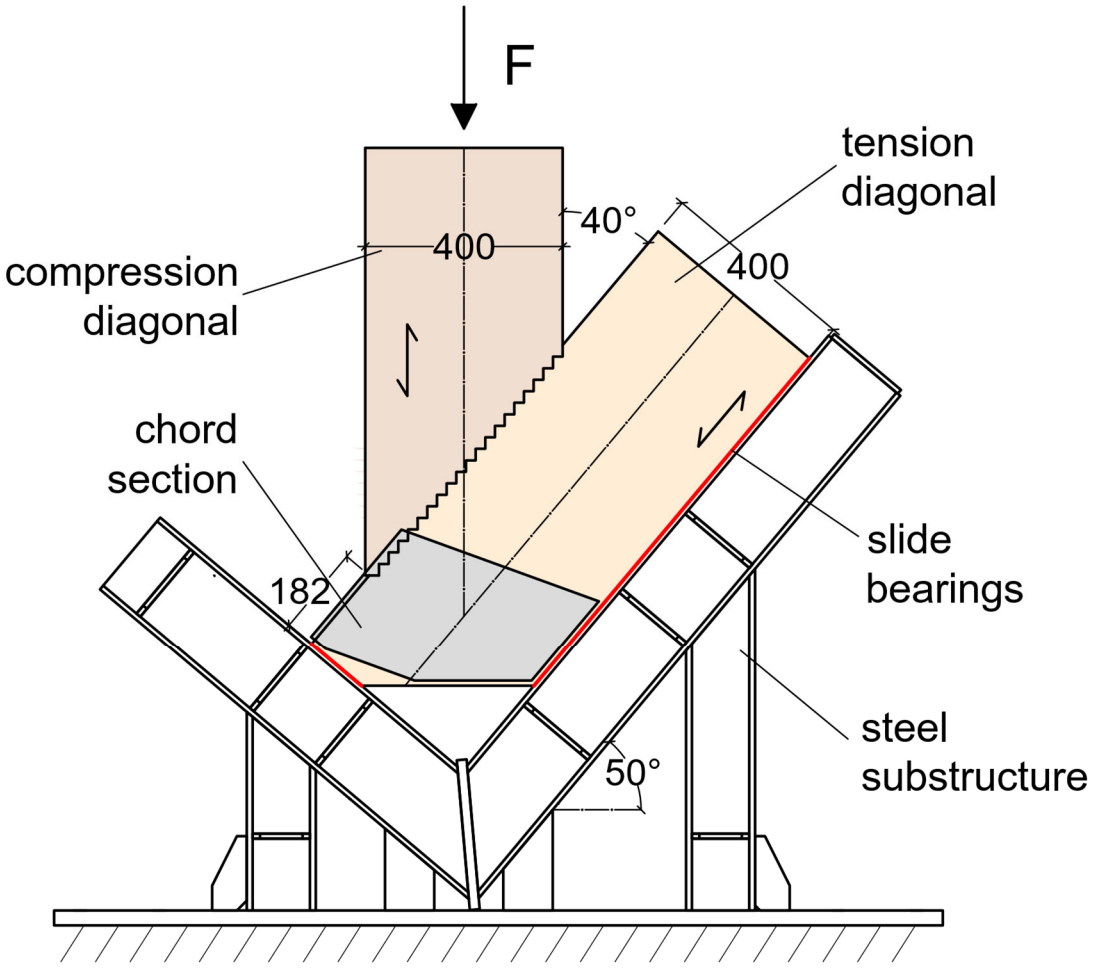

Fig. 5: Experimental test setup for a compression-shear test of the contact connection

Fig. 6: Realized experimental test setup for the compression-shear test of the contact connection

4. TEST RESULTS

4.1 Load Bearing Capacity

For all specimens of all series shear failures in the LVL of the tensional diagonal component in the vicinity of the multiple step joint could be observed. The average maximum load for the series with standard geometry was $F_{max,mean}$ = 413 kN. In comparison, the two alternative geometries, Modified 1 and 2, achieved average maximum loads of $F_{max,mean}$ = 485 kN and $F_{max,mean}$ = 490 kN, respectively, representing an increase of 17 – 19 %. The series Modified 1 and 2 in particular show a low scattering with a coefficient of variance of COV = 2.3 % and COV = 4.2 %, respectively. The COV of the Standard series is COV = 8.7 %.

An overview of the results is given in Table 1. The shear strengths are calculated by the shear force and a shear surface of A = 87080 mm², which corresponds to the shear length along the connection of the multiple step joint and the component depth. Additionally, the compression stresses perpendicular to the grain in the contact area of the tension diagonal were calculated from the lateral compression force, the length of the contact area and the depth of the GLVL-component. The forces for shear and lateral compressive loads were determined from fracture loads using the respective angle ratios. The mean shear strength resulted in $f_{v,mean}$ = 3.6 N/mm² for the Standard series and $f_{v,mean}$ = 4.3 N/mm² for the Modified 1 and 2 series. The mean compression stresses perpendicular to the grain were $z_{c,90,mean}$ = 3.0 N/mm² and $z_{c,90,k}$ = 3.6 N/mm², respectively.

To enhance comparability, also due to different number of specimens in the test series, for the calculation of characteristic values a fictive COV of 10 % and a k_s-value of 1.93, corresponding to a fictive number of 20 specimens were used [5]. This lead to a characteristic shear strength of $f_{v,k}$ = 2.9 N/mm² for the Standard series and $f_{v,k}$ = 3.5 N/mm² for both Modified series. The lateral compression stresses perpendicular to grain at the characteristic level of maximum loads were calculated equivalent to $z_{c,90,k}$ = 2.5 N/mm² and $z_{c,90,k}$ = 2.9 N/mm², respectively.

The characteristic shear strength of all series exceeds the specified shear strength of LVL (Kerto S) of $f_{v,k}$ = 2.3 N/mm², according to [6], by 26 % and 52 %. This can most likely be attributed to a positive interaction of shear and perpendicular to the grain stresses [7]. Moreover, there is an additional effect of the optimised geometry of the modified series leading to a more efficient load introduction to the tension diagonal.

The lateral compression stresses (at the characteristic level of fracture loads) of $z_{c,90,k}$ = 2.5 N/mm² and $z_{c,90,k}$ = 2.9 N/mm² also exceed the specified lateral compression strength of LVL (Kerto S) of $f_{c,90,k}$ = 2.2 N/mm², however without resulting in any noticeable failure.

Table 1: Averaged maximum loads and corresponding shear strength and lateral compression stresses

Test series	Maximum load	Shear strength		Lateral compression stresses		n
	$F_{max,\,mean}$ [kN]	$f_{v,mean}$ [N/mm²]	$f_{v,k}$ [N/mm²]	$z_{c,90,mean}$ [N/mm²]	$z_{c,90,k}$ [N/mm²]	[-]
Standard	413	3.6	2.9	3.0	2.5	5
Modified 1	485	4.3	3.5	3.6	2.9	4
Modified 2	490	4.3	3.5	3.6	2.9	6

4.2 Failure Modes

The load-displacement curves of all series are shown in Fig. 7. Both modified series, Modified 1 and 2 show a significantly less brittle behaviour compared to the Standard series. While the specimens from the Standard series exhibit an immediate load drop after reaching the F_{max} without significant recovery, all specimens from the Modified series show a quasi-ductile behaviour, partially maintaining a high load level (ca. 60 – 80 % F_{max}) after reaching the maximum load.

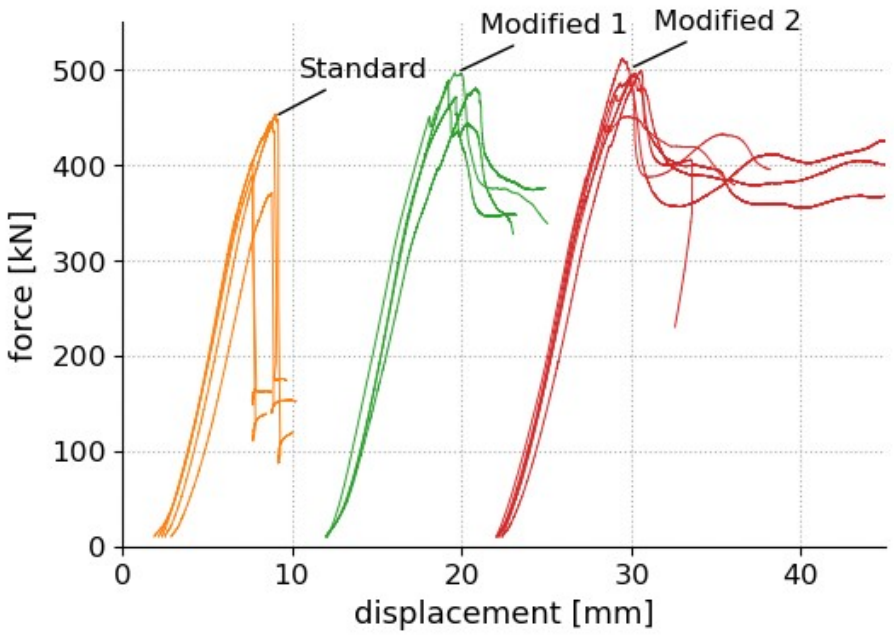

Fig. 7: Load-displacement curves for the specimens of series Standard, Modified 1 and 2

The discussed load-displacement behaviour is mirrored by the damage/crack propagation behaviour observed during the tests and by the visible crack pattern after failure. For the specimens of the Modified 1 series, several – well separated – failure planes in several veneer layers in the LVL material of the tension diagonal are visible. In the steps on the side of the compression diagonal (i.e. in the glulam), considerable splitting was observed. This was probably initiated by the shear cracks within the LVL, whereby the induced non-linear deformations are transferred to the glulam counterpart by frictional locking causing stresses perpendicular to the grain in the glulam and subsequent splitting (see Fig: 9a). Series Modified 2 showed similar failure behaviour with even more pronounced splitting phenomena (see Fig: 9b). In contrast, specimens of the standard series mainly showed shear failure along one or few closely spaced veneer layers, primarily located at the tips of the steps (see Fig. 8).

Fig. 8: Representative failure mode observed in the multiple step joints of specimen from the Standard series; shear failure cracks are highlighted with dotted lines

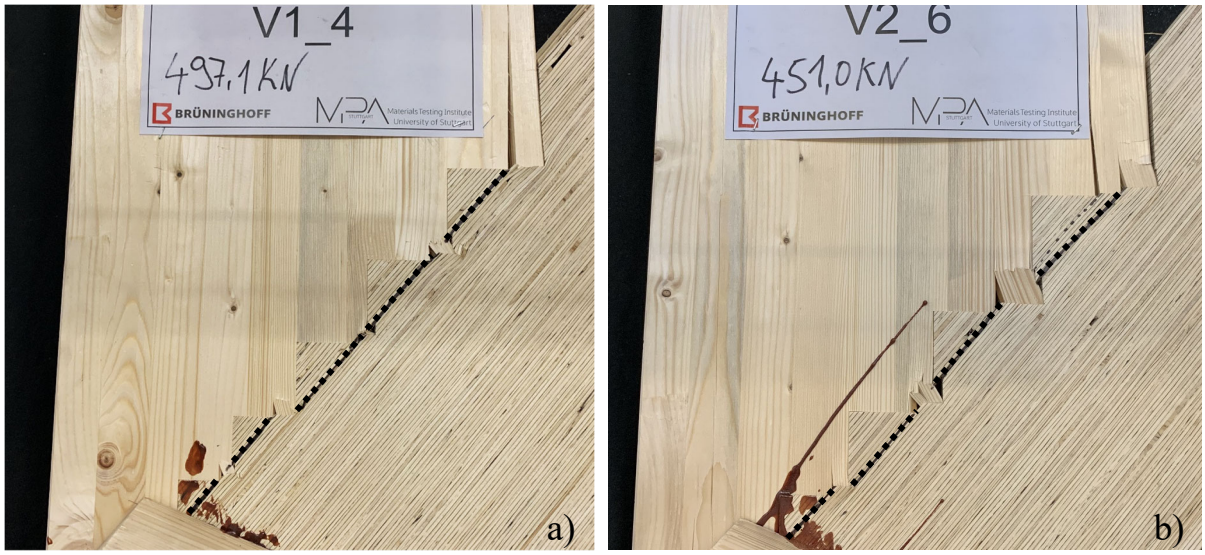

Fig: 9: Representative failure modes observed in the multiple step joints of specimen from the modified series Modified 1 (a) and Modified 2 (b); shear failure cracks are highlighted with dotted lines

5. DISCUSSION

Clear shear failures were observed in both, the standard and the modified series. Since the load-bearing capacity of the modified series was significantly improved, it can be concluded that this improvement is due to an increase in the effective shear capacity of the connection.

Based on the observed failure modes in the standard series, the veneer layer at the step tip of each step experiences the highest load and is primarily responsible for connection failure. Consequently, the load-bearing capacity is largely dependent on a single veneer layer of the LVL. By varying the embedment depths, multiple – well separated – veneer layers are activated, increasing the redundancy of the connection. Although the coefficient of variation is relatively low (standard series: COV ≈ 9 %), it further decreases for the modified series (COV < 5 %)

Since the coefficients of variation COV is also low for the standard series, redundancy alone cannot fully explain the increased shear strength observed in the modified series. It is likely that the adapted geometry results in the activation of the shear area by engaging multiple veneer layers. However, the number of individual steps and the difference between embedment depths of 57 mm and 70 mm (i.e. transition from Modified 1 to Modified 2) seem to have no further significant influence.

The results of the FE-based investigation showed no significant influence regarding shear stresses along the connection when comparing compression- and tension-based support, which induces compression and tension forces in the tension diagonal, respectively. However, since the FE-model uses a simplified geometry without modelling the individual steps, the particular influence of the individual steps cannot be assessed from this analysis.

The steps of the connection act as notches, resulting in tension stresses perpendicular to the grain in the edges. These stresses are highest at the outermost step with the greatest embedment depth. In contrast to the realized test setup, where compression forces act in the tension diagonal, tension forces in this diagonal would also result in compression perpendicular to the grain along the connection, but not at the most stressed, outermost edge. Consequently, the tension stresses perpendicular to the grain in this area are not compensated by the compressive stresses perpendicular to the grain from lateral compression forces. Assumingly, in the realized tests the acting compression in the entire diagonal can prevent failure due to tension stresses perpendicular. Under tensile loads, however, the area at the first step could potentially initiate premature failure.

This effect occurs also in the standard series, but to a lesser extent as the embedment depth is much lower.

6. CONCLUSION

The characteristic effective shear strengths from all series are higher than the declared shear strength of LVL assumingly due to the positive effect of interaction between shear and lateral compression. Additionally, the results show that the varying embedment depths of the individual steps result in a greater activation of the shear planes due to the activation of various, well separated veneer layers. Therefore, the load bearing capacity and at the same time the redundancy of the modified geometries could be improved compared to the geometry of the standard series. At the same time no significant difference between the two modified series could be observed.

The effect of a notch under pure tensile stress in the tension diagonal, which results in tensile stresses perpendicular to the grain at the edge of the notch, cannot be addressed in these tests and requires further detailed investigations.

ACKNOWLEDGEMENTS

The close cooperation in the R&D project and the subsequent approval investigations with company Brüninghoff Holz GmbH & Co. KG, is gratefully acknowledged. All specimens and some part of the testing equipment (i.e. the special steel frame) were designed and developed jointly and have been produced and made available by the Brüninghoff Group.

REFERENCES

[1] Z-9.1-847: *Bauarten mit Furnierschichtholz "Kerto LVL S-beam", "Kerto LVL Q-panel" und "Kerto LVL Qp-beam"– Allgemeine bauaufsichtliche Zulassung*, Berlin, Deutschen Institut für Bautechnik, 2024

[2] EN 14080: *Timber structures – Glued laminated timber and glued solid timber - requirements*, Brussels, European Committee for Standardization, 2013

[3] ENDERS-COMBERG, M.: *Leistungsfähige Verbindungen im Ingenieurholzbau – Einsatzmöglichkeiten für Nadel- und Laubholz, Karlsruher Institut für Technologie (KIT),* Karlsruhe, 2015

[4] ABAQUS: *ABAQUS/Standard user's manual, version 2023*, Providence, RI, USA: Dassault Systèmes, 2020

[5] EN 14358: *Timber structures – Calculation and verification of characteristic values*, Brussels, European Committee for Standardization, 2017

[6] Z-9.1-100: *Kerto Furnierschichtholz– Allgemeine bauaufsichtliche Zulassung*, Berlin, Deutschen Institut für Bautechnik, 2021

[7] STEIGER, R.; GEHRI, E.: *Interaction of shear stresses and stresses perpendicular to the grain, In: Proceedings of CIB-W18, Meeting 44, Alghero, 2011*